Extended X-Ray Absorption Fine Structure Studies of Transition-metal Periodate and Tellurate Complexes. Crystal Structure of $Rb_2Na_4[OsO_2(H_2TeO_6)_2]\cdot 16H_2O$†

William Levason,* Richard D. Oldroyd and Michael Webster
Department of Chemistry, University of Southampton, Southampton SO17 1BJ, UK

The structures of a range of transition-metal (Cu, Ag, Au, Ru, Os, Pd, Pt, Co and Mn) periodate or tellurate complexes have been determined using a combination of metal K- or L_{III}-edge and iodine or tellurium K-edge extended X-ray absorption fine structure data. The crystal structure of the osmium(VI) tellurate $Rb_2Na_4[OsO_2(H_2TeO_6)_2]\cdot 16H_2O$ has been determined and contains OsO_6 and TeO_6 octahedral groups linked *via* edge sharing to form a discrete anion.

Periodate $[H_{5-n}IO_6]^{n-}$ and tellurate $[H_{6-n}TeO_6]^{n-}$ ions behave as chelating O-donor ligands towards many transition and some p-block metals. We have previously reported[1-3] the use of a combination of multi-edge extended X-ray absorption fine structure (EXAFS) and powder X-ray diffraction data to establish the structures of the insoluble $MM'IO_6$ (M = alkali metal; M' = Ni, Mn, Ge, Sn or Pb), which have extended layer structures. A variety of water soluble bis- and tris-(ligand) complexes are also known and the structures of several of these have been established by single crystal X-ray work.[1,4-13] These complexes often contain unusually high oxidation states of the metals, in discrete water soluble anions, and have uses as specific oxidants and in analysis.[8,12] However single crystals of these complexes are difficult to obtain, often requiring mixed cations, and here we report attempts to obtain structural data using a combination of tellurium or iodine K-edge and metal K- or L_{III}-edge EXAFS data.

Experimental

EXAFS measurements were made at the Daresbury Synchrotron Radiation Source, operating at 2 GeV (*ca.* 3.2×10^{-10} J) with typical currents of 200 mA. Iodine and tellurium K-edge data were collected on station 9.2 using a channel-cut silicon(220) monochromator. Palladium, ruthenium and silver K-edge data were also obtained on station 9.2 using a double-crystal silicon(220) monochromator. Copper, manganese and cobalt K-edge and platinum, osmium and gold L_{III}-edge data were obtained on station 7.1 using a silicon(111) order-sorting monochromator. Data were collected in transmission mode from samples diluted with boron nitride and mounted between Sellotape in 1 mm aluminium holders.

The complexes were prepared by literature methods[4-6,8,11,14-16] and the heavy-atom ratios checked by energy-dispersive X-ray (EDX) analysis using a JEOL JSM6400 scanning electron microscope operating with a 20 keV (*ca.* 3.2×10^{-15} J) electron energy, and fitted with a Tracor Northern series 2 X-ray and image analyser.

X-Ray Crystallographic Study of $Rb_2Na_4[OsO_2(H_2TeO_6)_2]\cdot 16H_2O$.—Brown crystals were obtained by slow evaporation from an aqueous solution containing rubidium, potassium and sodium hydroxide together with the sodium salt of the osmium tellurate anion, and sealed in glass capillaries for X-ray examination. EDX measurements on the crystals showed the presence of rubidium, tellurium, osmium, sodium and essentially no potassium.

Crystal data. $H_{36}Na_4O_{30}OsRb_2Te_2$, M = 1224.6, monoclinic, space group $C2/c$, a = 10.737(3), b = 25.333(4), c = 10.910(3) Å, β = 108.51(2)°, U = 2813.9 Å^3, Z = 4, D_c = 2.890 g cm^{-3}, $F(000)$ = 2296, λ = 0.710 69 Å, μ = 100.6 cm^{-1}.

Data collection. Data were collected using an Enraf–Nonius CAD-4 diffractometer equipped with Mo-Kα radiation and a graphite monochromator. Cell dimensions were obtained from 25 reflections ($13 < \theta < 15°$) and a room temperature crystal (0.4 × 0.4 × 0.25 mm). From the same crystal, 2990 reflection intensities were measured ($1 < \theta < 26°$, h 0–13, k 0–31, l −13 to 12) and after averaging there remained 2767 unique reflections (R_{int} = 0.029). The Lorentz-polarisation correction was applied together with a ψ-scan empirical absorption correction (maximum and minimum transmission factors 99.9 and 30.7) and no crystal decay was noted in the check reflection. 2426 Reflections with $F > 2\sigma(F)$ were used in the analysis and refinement. The systematic absences established the space group as Cc or $C2/c$ and the latter was confirmed by the structure solution.

Structure solution and refinement. The Te and Os atom positions are on the two-fold axis and were located using SHELXS 86.[17] Subsequent structure factor and electron-density calculations gradually gave the position of the Rb, Na and O atoms. After allowing the atoms to have anisotropic thermal parameters and after least-squares refinement, seven reflections were removed due to possible extinction/poor agreement. No convincing evidence for hydrogen atoms appeared in the later electron-density maps and no attempt was made to introduce them into the model. Full-matrix least-squares refinement using SHELX 76[18] converged to R = 0.036 [180 parameters, 2419 reflections, all atoms anisotropic, maximum shift/error = 0.1, $w^{-1} = \sigma^2(F) + 0.0005F^2$, R' = 0.051]. The residual electron density was in the range 2.42 to −3.55 e Å^{-3}. Complex atomic scattering factors were taken from ref. 19 (Os, Te, Na, Rb) and SHELX 76 (O)[18] and all calculations were carried out using the programs SHELXS 86,[17] SHELX 76[18] and PLUTO[20] on a personal computer. A list of atomic coordinates is presented in Table 1 and Table 2 records bond lengths and angles.

Additional material available from the Cambridge Crystallographic Data Centre comprises thermal parameters and remaining bond lengths and angles.

EXAFS Refinements.—The raw data were background

† *Supplementary data available:* see Instructions for Authors, *J. Chem. Soc., Dalton Trans.*, 1994, Issue 1, pp. xxiii–xxviii.

Table 1 Atomic coordinates for $Rb_2Na_4[OsO_2(H_2TeO_6)_2]\cdot16H_2O$

Atom	*x*	*y*	*z*
Os(1)	0.0000	0.279 76(1)	0.2500
Te(1)	0.0000	0.156 77(2)	0.2500
Te(2)	0.0000	0.402 63(2)	0.2500
Rb(1)	0.145 09(8)	0.045 20(3)	0.476 32(7)
Na(1)	0.5000	0.837 7(2)	0.7500
Na(2)	0.5000	0.574 4(2)	0.7500
Na(3)	0.5000	0.705 9(2)	0.7500
Na(4)	0.5000	0.969 3(2)	0.7500
O(1)	0.102 3(6)	0.279 5(2)	0.410 8(5)
O(2)	0.097 5(5)	0.217 3(2)	0.211 1(5)
O(3)	0.121 3(5)	0.159 8(2)	0.430 9(5)
O(4)	0.103 9(5)	0.108 4(2)	0.201 0(5)
O(5)	0.098 3(5)	0.342 3(2)	0.213 4(5)
O(6)	0.115 1(5)	0.398 5(2)	0.432 4(4)
O(7)	0.106 1(5)	0.451 5(2)	0.207 3(5)
O(8)	0.131 8(5)	0.139 7(2)	0.691 5(5)
O(9)	0.134 0(5)	0.404 4(2)	−0.301 6(5)
O(10)	0.133 4(5)	0.272 3(2)	−0.308 0(6)
O(11)	0.125 7(7)	0.214 0(2)	0.970 7(6)
O(12)	0.112 6(6)	0.074 6(2)	0.974 4(5)
O(13)	0.132 4(6)	0.335 7(3)	−0.026 3(6)
O(14)	0.149 0(5)	−0.005 3(2)	0.229 6(5)
O(15)	−0.122 5(7)	0.539 8(4)	0.022 7(6)

Table 2 Selected bond lengths (Å) and angles (°) for $Rb_2Na_4[OsO_2(H_2TeO_6)_2]\cdot16H_2O$

Te(1)–O(2)	1.978(5)	Te(2)–O(5)	1.968(4)
Te(1)–O(3)	1.991(5)	Te(2)–O(6)	1.984(4)
Te(1)–O(4)	1.847(5)	Te(2)–O(7)	1.840(5)
Os(1)–O(1)	1.750(5)	Te(1) · · · Os(1)	3.116(1)
Os(1)–O(2)	2.015(5)	Te(2) · · · Os(1)	3.113(1)
Os(1)–O(5)	2.013(5)		
	Na(1) · · · O	2.400(6)–2.404(6)	
	Na(2) · · · O	2.361(6)–2.429(6)	
	Na(3) · · · O	2.366(6)–2.420(6)	
	Na(4) · · · O	2.368(6)–2.425(6)	
	Rb(1) · · · O	2.834(5)–3.387(5)	
O(2)–Te(1)–O(3)	87.6(2)	O(5)–Te(2)–O(6)	87.6(2)
O(2)–Te(1)–O(4)	92.5(2)	O(5)–Te(2)–O(7)	93.2(2)
O(3)–Te(1)–O(4)	92.7(2)	O(6)–Te(2)–O(7)	93.0(2)
O(2)–Te(1)–O(2a)	78.3(3)	O(5)–Te(2)–O(5a)	78.2(3)
O(3)–Te(1)–O(3a)	175.6(3)	O(6)–Te(2)–O(6a)	173.9(3)
O(4)–Te(1)–O(4a)	96.9(3)	O(7)–Te(2)–O(7a)	95.4(3)
O(1)–Os(1)–O(2)	90.3(2)	O(1)–Os(1)–O(1a)	179.5(3)
O(1)–Os(1)–O(5)	90.0(2)	O(2)–Os(1)–O(2a)	76.6(3)
O(2)–Os(1)–O(5)	103.7(2)	O(5)–Os(1)–O(5a)	76.1(3)

Symmetry code: a = $-x,y,\frac{1}{2}-z$.

subtracted using the program PAXAS[21] by fitting a 6 or 8 order split polynomial to the pre-edge subtracted spectrum between k = 2 Å^{-1} up to 12–13 Å^{-1} in most cases for the I and Te edges, and up to 15 Å^{-1} for the metal edges. Curve fitting was carried out using the program EXCURVE 92.[22] Ground state potentials of the atoms were calculated using Von Barth theory and phase shifts using Hedin–Lundqvist potentials. The metal-edge data refinements were straightforward, two shells being fitted for all of the complexes, with the exception of those of ruthenium and osmium where three shells were modelled. The distances and the Debye–Waller factors were refined for all the shells, as well as the Fermi energy difference. The occupancy of the M–E (E = Te or I) shell was varied to determine the best fit on the basis of the lowest fit index. In all cases the number of E atoms calculated was the same as the number expected from the crystal structures.

The iodine and tellurium K-edge data were more difficult to fit due to the different I–O and Te–O bond distances that occur in these complexes. Phase shifts and amplitude-reduction

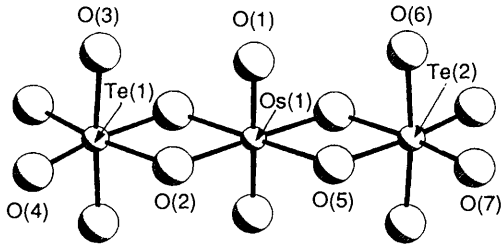

Fig. 1 Structure of the anion in $Rb_2Na_4[OsO_2(H_2TeO_6)_2]\cdot16H_2O$ showing the atom labelling

factors were checked using KIO_4 and $Te(OH)_6$ as models, and the complexes were initially modelled using a first shell of six oxygens and a second shell of the appropriate number of metal atoms. The first oxygen shell was then split into two where occupancies of the short and long distances were changed from 4/2 to 3/3 to 2/4. Due to initial problems with high correlations between the Debye–Waller factors and the bond distances, the Debye–Waller factor of the first (short) shell was set at 0.0020 for the periodates, in line with the value calculated for KIO_4 which has four I=O double bonds, and was not refined with the other variables. The same value was used for the tellurates as the complexes with known crystal structure compared much better using this value rather than setting the Debye–Waller of the longer shell to the value calculated for $Te(OH)_6$. The act of including the extra shell was checked for statistical significance[23] and the number of independent data points (N) in all cases was greater than the number of variables refined ($N = 2\Delta k\Delta R/\pi$).[23]

Results and Discussion

Structure of $Rb_2Na_4[OsO_2(H_2TeO_6)_2]\cdot16H_2O$.—The structure consists of the $[OsO_2(H_2TeO_6)_2]^{6-}$ anion (Fig. 1) and hydrated Na and Rb cations; bond lengths are reported in Table 2. A unit-cell packing diagram is shown in Fig. 2. The anion has crystallographic two-fold symmetry with the Os and Te atoms lying on the two-fold axis and as the H atoms were not located the degree of protonation is inferred from the Te–O bond lengths and supported by IR data. Where H atoms have been located in periodates,[1,5] the I–O(H) is longer than the terminal I–O distance and thus we regard O(3) and O(6) as O(H) groups. The Te–O distances are in accord with those found in $K_6Na_2[Pt(OH)_2(HTeO_6)_2]\cdot12H_2O$ (1.87–2.08 Å).[4] The terminal Os–O distance [1.750(5) Å] may be compared with 1.718(4) Å found[24] in the $[OsO_2Cl_4]^{2-}$ anion. The sodium ions are surrounded by six O atoms in an approximately octahedral arrangement [Na · · · O 2.361(6) to 2.429(6) Å] with the O atoms arising from the water molecules although O(7) is involved with Na(4). The rubidium is surrounded by ten O atoms [Rb · · · O 2.834(5) to 3.387(5) Å] in an irregular polyhedron with distances similar to those found recently[25] in $Rb_6[TeMo_6O_{24}]\cdot10H_2O$ and $Rb_6[TeMo_6O_{24}]\cdot Te(OH)_6\cdot6H_2O$ where 8-, 9- and 10-co-ordinate Rb ions were found with the shortest Rb · · · O of 2.830(7) Å. It is noteworthy that repeated attempts to prepare single crystals of the anion with a single cation invariably yielded fine powders and only when mixed cations were employed were suitable crystals formed. This has been commented on previously[4,5] and a mixed-cation synthetic strategy should be tried early on in crystal-growing experiments.

EXAFS.—Metal K- *and* L_{III}-*edge data.* The treatment of the metal K- and L_{III}-edge data was straightforward, the observed EXAFS data being satisfactorily modelled by shells corresponding to oxygen atoms in the first co-ordination sphere of the metal, and to the (non-bonded) iodine or tellurium. No other significant features were present. Table 3 summarises the results obtained, and compares them with single-crystal X-ray data

Table 3 Metal K- and L_{III}-edge EXAFS and X-ray crystallographic data

Anion	d(M–O)[a]/Å	$2\sigma^2$[b]/Å^2	d(M–O)[c]/Å	d(M–E)[d]/Å	$2\sigma^2$/Å^2	d(M–E)[c]/Å	F.i.[e]	R[f] (%)
$[Cu\{TeO_4(OH)_2\}_2]^{5-}$	1.823(2)	0.0064(4)	1.836(3)[g]	2.907(1)	0.0057(2)	2.881(1)[g]	3.7	24.8
$[Ag\{TeO_4(OH)_2\}_2]^{5-}$	1.975(2)	0.0035(3)	—	3.023(1)	0.0049(2)	—	3.7	20.7
$[Au\{TeO_4(OH)_2\}_2]^{5-}$	1.978(2)	0.0052(3)	—	3.028(2)	0.0055(2)	—	3.3	24.6
$[RuO_2\{TeO_4(OH)_2\}_2]^{6-}$	1.734(2)	0.0008(3)	—	3.035(2)	0.0046(2)	—	2.8	22.5
	2.044(2)	0.0040(3)						
$[OsO_2\{TeO_4(OH)_2\}_2]^{6-}$	1.748(2)	0.0042(5)	1.750(5)[h]	3.099(2)	0.0051(2)	3.115(2)[h]	4.8	29.5
	2.023(2)	0.0056(4)	2.014(1)					
$[Pt(OH)_2\{TeO_5(OH)\}_2]^{8-}$	1.999(1)	0.0047(2)	2.015(2)[i]	3.021(1)	0.0042(2)	3.065(1)[i]	2.1	18.4
$[Pd_2Te_4O_{24}H_2]^{14-}$ (dimer)	1.993(2)	0.0036(2)	1.996(22)[i]	3.046(2)	0.0067(2)	3.064(30)[i]	2.9	20.5
(monomer)	1.993(2)	0.0036(2)		3.046(2)	0.0036(2)		3.3	22.0
$[Cu\{IO_5(OH)\}_2]^{5-}$	1.822(2)	0.0041(3)	1.835(18)[j]	2.895(1)	0.0036(2)	2.912(28)[j]	3.5	24.2
$[Ag\{IO_5(OH)\}_2]^{5-}$	1.978(2)	0.0036(2)	1.979(11)[k]	3.019(1)	0.0050(2)	3.020(3)[k]	3.1	18.2
$[Au\{IO_5(OH)\}_2]^{5-}$	1.959(2)	0.0049(3)	1.977(2)[l]	3.028(1)	0.0041(2)	3.034(1)[l]	3.5	25.4
$[RuO_2\{IO_5(OH)\}_2]^{6-}$	1.748(2)	0.0020(4)	1.732(8)[m]	3.101(2)	0.0024(2)	3.093(1)[m]	4.1	26.8
	2.023(2)	0.0035(4)	2.012(4)[m]					
$[OsO_2\{IO_5(OH)\}_2]^{6-}$	1.756(4)	0.0049(9)	—	3.108(2)	0.0023(2)	—	7.2	31.5
	2.007(3)	0.0043(6)						
$[Pt(OH)_2\{IO_5(OH)\}_2]^{6-}$	1.990(8)	0.0079(4)	1.996(5)[n]	3.038(2)	0.0042(3)	3.049(1)[n]	4.0	20.9
$[Pd_2I_4O_{24}H_2]^{10-}$ (dimer)[o]	1.995(2)	0.0038(3)	—	3.049(3)	0.0093(5)		3.2	22.9
(monomer)	1.989(2)	0.0037(3)	—	3.041(2)	0.0041(3)		4.4	26.6
$[Mn\{IO_5(OH)\}_2\{IO_4(OH)_2\}]^{7-}$	1.901(4)	0.0017(4)	1.903(38)[p]	2.946(2)	0.0036(4)	2.957(2)[p]	9.3	22.7
$[Co_4I_3O_{24}H_{12}]^{3-}$[q]	1.892(17)	0.0057(3)	1.91(26)[r]	2.952(5)	0.0108(8)	2.955(43)[r]	3.2	19.9

[a] Standard deviations in parentheses. Note that the systematic errors in bond distances arising from the data collection and analysis procedures are *ca.* ±0.02–0.03 Å for well defined co-ordination shells and ±0.03 Å for more remote shells. [b] Debye–Waller factor. [c] X-Ray crystallographic data from references cited. [d] Non-bonded distance E = I or Te, with co-ordination numbers fixed as required by the structures in Fig. 3. [e] Fit index defined as $\Sigma_i[(\chi^T - \chi^E)k_i^3]^2$. [f] R factor defined as $[\int(\chi^T - \chi^E)k^3dk/\int\chi^Ek^3dk] \times 100$. [g] Ref. 6. [h] This work. [i] Ref. 4. [j] Ref. 7. [k] Ref. 9. [l] Ref. 12. [m] Ref. 8. [n] Ref. 5. [o] d(Pd···Pd) 2.819(6) Å, $2\sigma^2$ = 0.0064(10) Å^2. [p] Ref. 1. [q] d(Co···Co) 2.847(3) Å [2.827(9) Å from crystal structure, ref. 11], $2\sigma^2$ = 0.0011(4) Å^2. [r] Ref. 11.

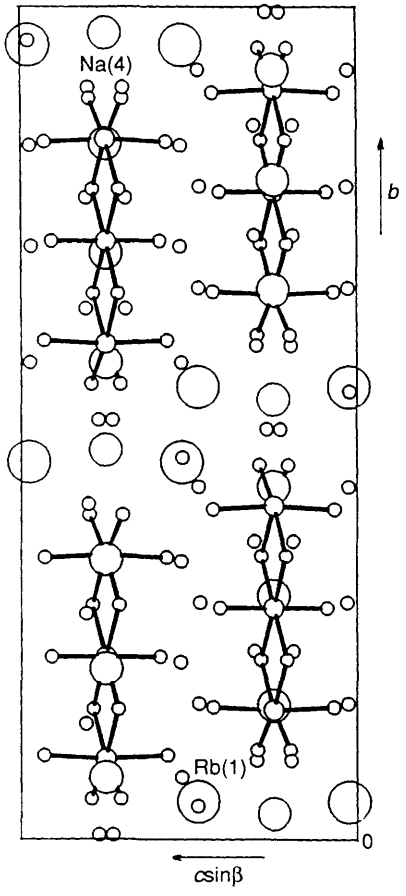

Fig. 2 Packing diagram for $Rb_2Na_4[OsO_2(H_2TeO_6)_2]\cdot16H_2O$ viewed down the *a* direction

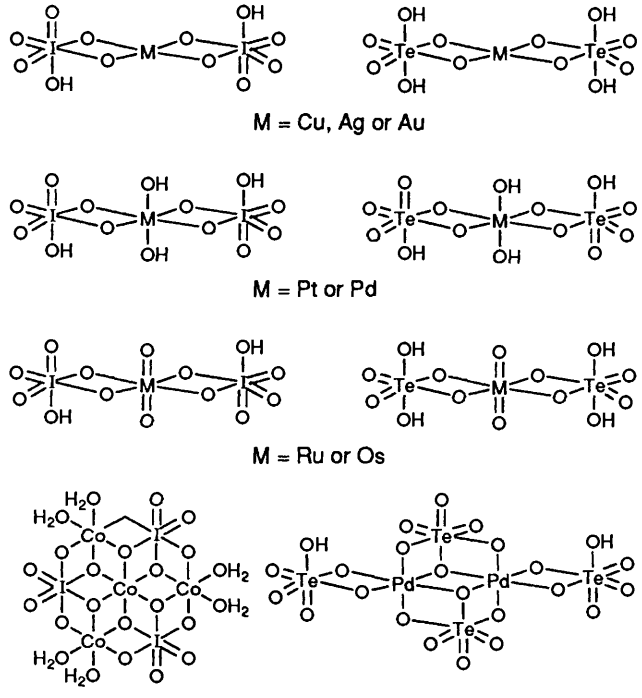

Fig. 3 Periodate and tellurate structural types

where the latter are available. The arrangement about the metal centre in the bis(ligand) species increases in complexity from the Group 11 complexes $[ML_2]^{5-}$ [M = Cu, Ag or Au; L = $TeO_4(OH)_2$ or $IO_5(OH)$], which contain planar four-co-ordinate metal centres, through $[Pt(OH)_2\{IO_5(OH)\}_2]^{6-}$ and $[Pt(OH)_2\{TeO_5(OH)\}_2]^{8-}$, which contain six-co-ordinate metal centres, to $[MO_2L_2]^{6-}$ (M = Ru or Os) where the metal is six-co-ordinate with two short M=O and four longer M–OI(Te) bonds (Fig. 3). One tris(periodate), $[Mn\{IO_5(OH)\}_2\{IO_4(OH)_2\}]^{7-}$ is included in Table 3. The agreements between the EXAFS and X-ray data are generally excellent, and for those

Table 4 Tellurium K-edge EXAFS and relevant crystallographic data[a]

Anion	d(Te–M)/Å	$2\sigma^2$/Å^2	d(Te–O)/Å		$2\sigma^2$/Å^2	d(Te–O)[b]/Å	F.i.	R (%)
$Te(OH)_6$	—	—		1.909(1)	0.0062(2)	1.913(6)[c]	2.7	18.0
$[TeO_2(OH)_4]^{2-}$	—	—	6 × O	1.937(2)	0.0079(3)	1.939(41)[d]	4.9	18.4
			2 × O	1.871(6)	0.0020	1.870(2)	4.5	18.4
			4 × O	1.968(3)	0.0031(6)	1.958(2)		
$[Cu\{TeO_4(OH)_2\}_2]^{5-}$	2.914(4)	0.0062(8)	6 × O	1.941(2)	0.0093(4)	1.927(55)[e]	5.1	19.7
			2 × O	1.879(6)	0.0020	1.853(4)	4.7	18.5
			4 × O	1.978(3)	0.0045(7)	1.965(20)		
$[Ag\{TeO_4(OH)_2\}_2]^{5-}$	3.022(4)	0.0064(7)	6 × O	1.938(2)	0.0092(4)		4.7	21.6
			2 × O	1.862(6)	0.0020		3.9	18.5
			4 × O	1.972(3)	0.0064(7)			
$[Au\{TeO_4(OH)_2\}_2]^{5-}$	3.046(15)	0.0143(29)	6 × O	1.931(2)	0.0092(3)		3.8	18.5
			2 × O	1.851(6)	0.0020		3.3	16.5
			4 × O	1.963(3)	0.0026(6)			
$[RuO_2\{TeO_4(OH)_2\}_2]^{6-}$	3.041(2)	0.0011(3)	6 × O	1.940(2)	0.0042(2)		3.1	15.6
			2 × O	1.898(5)	0.0020		2.9	15.4
			4 × O	1.973(2)	0.0027(7)			
$[OsO_2\{TeO_4(OH)_2\}_2]^{6-}$	3.116(5)	0.0050(9)	6 × O	1.937(2)	0.0075(3)	1.935(65)[f]	3.1	16.2
			2 × O	1.862(6)	0.0020	1.844(4)	2.7	15.2
			4 × O	1.966(2)	0.0018(6)	1.980(8)		
$[Pt(OH)_2\{TeO_5(OH)\}_2]^{8-}$	3.029(4)	0.0027(5)	6 × O	1.943(3)	0.0052(4)	1.935(76)[g]	7.8	25.6
			3 × O	1.901(7)	0.0020	1.869(2)	7.6	25.5
			3 × O	1.976(3)	0.0026(11)	2.001(53)		
$[Pd_2Te_4O_{24}H_2]^{14-}$ (dimer)	3.072(3)	0.0069(5)	6 × O	1.939(3)	0.0090(4)	1.902(24)[g]	5.5	19.1

[a] See footnotes to Table 3. In the two-shell (2 O, 4 O) model the Debye–Waller parameter of the first shell was fixed at 0.002. [b] X-Ray crystallographic data from references cited. [c] Ref. 26. [d] Ref. 27. [e] Ref. 6. [f] This work. [g] Ref. 4.

complexes lacking X-ray data, the EXAFS data can be viewed with some confidence.

Tellurium and iodine K-edge data. The iodine K-edge data on the layer periodates $MM'IO_6$ (M = alkali metal; M′ = Ge, Sn, Pb, Mn or Ni) which contain regular IO_6 octahedra with each oxygen co-ordinated to one M′ have been described previously.[1–3] The present complexes are a more difficult problem in that three different oxygen environments are found, I(Te)=O, I(Te)–O–M and I(Te)–O–H, with the I(Te)–O distances spread over ≤0.25 Å. Initially the data were fitted to a first shell of six oxygens and second shell of one (non-bonded) metal, and then the effect of splitting the oxygen shell into two [short and long I(Te)–O bonds with occupation numbers ranging from 4/2, 3/3 and 2/4] examined. The non-bonded I(Te) • • • M distances were insensitive to the treatment of the I(Te)–O shell(s) and were in agreement with the values determined from the metal-edge data to the usual level of precision (≤ ±0.03 Å for more remote shells, see Table 3).

The tellurium K-edge data for $Te(OH)_6$ refined to place Te–O at 1.91 Å in excellent agreement with the X-ray crystallographic value[26] of 1.913(6) Å, and confirm the reliability of the treatment and of the phase shifts used. The data on the anion $[TeO_2(OH)_4]^{2-}$ which contains two short and four longer Te–O bonds were fitted both to a single shell of 6 × O and to two shells (short Te–O : long Te–O 4 : 2, 3 : 3, 2 : 4). The best fit was for the 2 : 4 model (Table 4) and this also gave the best agreement with the crystallographic data.[27] A similar approach was then applied to the tellurate complexes, and the models derived from a single oxygen shell and the best of the split-shell models are given in Table 4, where the bond lengths obtained are compared with available X-ray data. On balance therefore it seems that the tellurium K-edge data of these tellurate complexes modelled with the split oxygen shell provide the most satisfactory descriptions of the structures.

The iodine K-edge data on the periodates were then treated in a similar manner, and selected results are given in Table 5. The EXAFS data on the model compounds $[IO_4]^-$ and $[IO_4(OH)_2]^{3-}$ (the latter fitted to four short I=O and two longer I–OH bonds) gave good agreement with the crystallographic data.[28,29] However attempts to fit the data on the metal periodates were much less successful. The problem arises in the fitting of the I–O shell(s), since the non-bonded

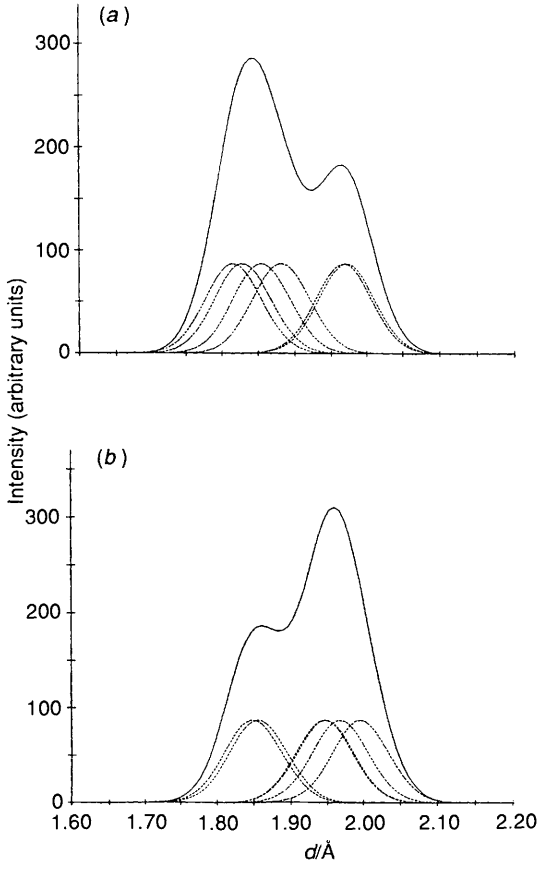

Fig. 4 Radial distribution functions of the first-shell oxygen atoms in (*a*) $[Au\{IO_5(OH)\}_2]^{5-}$ with iodine as the central atom and (*b*) $[Cu\{TeO_4(OH)_2\}_2]^{5-}$ with tellurium as the central atom

Table 5 Iodine K-edge EXAFS and relevant crystallographic data[a]

Anion	d(I–M)/Å	$2\sigma^2$/Å^2	d(I–O)/Å		$2\sigma^2$/Å^2	d(I–O)[b]/Å	F.i.	R(%)
$[IO_4]^-$	—	—	4 × O	1.766(2)	0.0020(2)	1.775(7)[c]	5.5	23.5
$[IO_4(OH)_2]^{3-}$	—	—	6 × O	1.837(2)	0.0081(4)	1.887(66)[d]	6.0	19.8
			4 × O	1.829(3)	0.0020	1.841(9)	3.9	15.1
			2 × O	1.954(6)	0.0049(8)	1.979(5)		
$[Au\{IO_5(OH)\}_2]^{5-}$	3.021(6)	0.0018(11)	6 × O	1.827(2)	0.0101(3)	1.887(62)[e]	3.3	16.9
			3 × O	1.789(6)	0.0020	1.833(16)	3.0	15.4
			3 × O	1.891(4)	0.0043(16)	1.941(42)		
$[Cu\{IO_5(OH)\}_2]^{5-}$	2.882(3)	0.0011(5)	6 × O	1.846(3)	0.0113(5)	1.904(69)[f]	6.2	20.4
$[Ag\{IO_5(OH)\}_2]^{5-}$	2.999(5)	0.0068(7)	6 × O	1.817(3)	0.0101(3)	1.905(74)[g]	5.1	23.5
$[RuO_2\{IO_5(OH)\}_2]^{6-}$	3.070(3)	0.0014(5)	6 × O	1.812(3)	0.0111(5)	1.890(77)[h]	6.1	24.2
$[OsO_2\{IO_5(OH)\}_2]^{6-}$	3.070(3)	0.0070(2)	6 × O	1.804(3)	0.0108(5)		6.0	21.7
$[Pt(OH)_2\{IO_5(OH)\}_2]^{6-}$	3.032(4)	0.0002(6)	6 × O	1.846(3)	0.0130(5)	1.894(82)[i]	4.8	21.1
$[Mn\{IO_4(OH)_2\}\{IO_5(OH)\}_2]^{7-}$	2.952(5)	0.0045(3)	6 × O	1.855(3)	0.0133(5)	1.887(67)[j]	7.5	21.5
$[Pd_2I_4O_{24}H_2]^{10-}$ (dimer)	3.017(3)	0.0048(5)	6 × O	1.827(3)	0.0120(5)	—	5.1	21.2
$[Co_4I_3O_{24}H_{12}]^{3-}$	2.898(3)	0.0048(4)	6 × O	1.833(3)	0.0130(6)	1.910(100)[k]	5.6	22.2

[a] See footnotes to Table 3. [b] X-Ray crystallographic data from references cited. [c] Ref. 28. [d] Ref. 29. [e] Ref. 12. [f] Ref. 7. [g] Ref. 9. [h] Ref. 8. [i] Ref. 5. [j] Ref. 1. [k] Ref. 11.

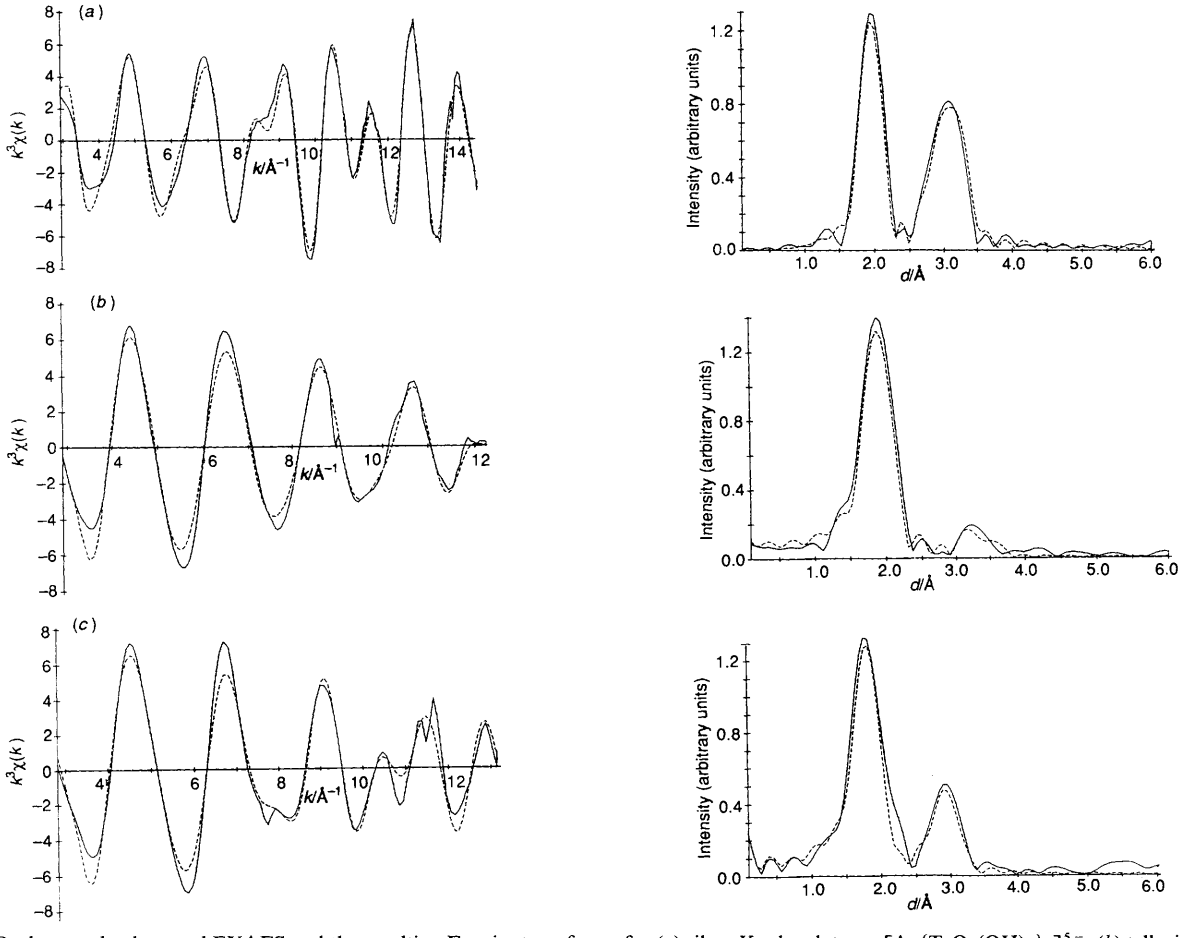

Fig. 5 Background-subtracted EXAFS and the resulting Fourier transforms for (*a*) silver K-edge data on $[Ag\{TeO_4(OH)_2\}_2]^{5-}$, (*b*) tellurium K-edge data on $[OsO_2\{TeO_4(OH)_2\}_2]^{6-}$ and (*c*) iodine K-edge data on $[Cu\{IO_5(OH)\}_2]^{5-}$. The full lines are experimental data, the broken lines theoretical plots in each case

M···I distances agree well with those from the metal-edge data and those obtained crystallographically. Examination of the single-crystal X-ray data available on several of the compounds reveals that there is a spread of I–O distances and that generally d(I=O), d(I–OM) and d(I–OH) do not fall into separate groupings as initially expected. Moreover the values are not symmetrically distributed about the average d(I–O). The EXAFS data treatment assumes a Gaussian distribution of d(I–O), and fails to treat satisfactorily the significantly non-Gaussian distributions as in these cases. Fig. 4(*a*) which shows a plot of the radial curves for each oxygen in the gold periodate complex* illustrates the problem, whilst Fig. 4(*b*) shows a similar plot for copper tellurate, from which it can be seen that the successful fitting (and splitting) of the oxygen shells in the tellurates is somewhat fortuitous, and is a result of the grouping of distances into short d(Te=O) and long d(Te–OH) and

* The crystal data[12] reveal six I–O distances, 1.972(4), 1.968(5), 1.882(4), 1.855(6), 1.829(4) and 1.816(5) Å.

d(Te–OM), and their relatively even distributions. The result of these non-Gaussian distributions of d(I–O) distances in the periodate complexes is to place the EXAFS determined d(I–O) at too short a value (by $\leqslant$0.1 Å).[30] Other models with split oxygen shells (long : short 4 : 2, 3 : 3, 2 : 4) were explored but gave no significant improvements, and in Table 5 the models resulting from a single (6 × O) first shell are given. Typical examples of background-subtracted EXAFS data and the corresponding Fourier transforms are shown in Fig. 5.

Dinuclear and cluster complexes. We have described elsewhere[5] how the metal-edge EXAFS data may be used to distinguish between bis-and tris-(periodate) complexes, and in the bis complexes between edge-bridging (η^2) and face-bridging (η^3) modes, in complexes containing a single metal centre. It was also of interest to see if the EXAFS data could identify larger groupings. The palladium(IV) tellurate,[4] $Na_8K_2H_4[Pd_2Te_4O_{24}H_2]$, is known from an X-ray study to have a dimeric tellurate-bridged structure (Fig. 3). The palladium and tellurium K-edge EXAFS data were fitted to both the dimer structure and to a monomer formulation $[Pd(OH)_2\{TeO_5(OH)\}_2]^{8-}$ analogous to the platinum complex. From the palladium K-edge results, a plot of the fit index *versus* the number of tellurium atoms showed a clear minimum at three consistent with the dimer structure, and the data resulting from the monomer and dimer models are given in Tables 3 and 4. The only problem with the dimer model was that attempts to fit a shell corresponding to the Pd ··· Pd distance resulted in high correlations with the Pd ··· Te shell, which is not surprising given the very similar distances. In view of the increasing complexity, the tellurium K-edge were fitted only to a two-shell (6 × O, 1.5 × Pd) model. The palladium(IV) periodate complex, analytically formulated as $K_6[Pd(OH)_2(HIO_6)_2]\cdot nH_2O$, has resisted all attempts to produce X-ray quality crystals, although powder X-ray diffraction studies showed that it is not isomorphous with (the structurally characterised) $K_6[Pt(OH)_2(HIO_6)_2]\cdot nH_2O$.[5] The palladium and iodine EXAFS data on this material have been modelled to both the monomer formula above and to a dimer $[Pd_2I_4O_{24}H_2]^{10-}$ (by analogy with the tellurate, although the degree of protonation is of course uncertain). The best fits are shown in Tables 3 and 5, and indicate that the material could well be dimeric in the solid state.

Finally cobalt and iodine K-edge data were recorded and modelled for the cobalt periodate cluster $H_3[Co_4I_3O_{24}H_{12}]$ (Fig. 3). Again, a reasonably good fit was obtained.

Acknowledgements

We thank Dr. D. C. Povey (University of Surrey) for the X-ray data collection, the Director of the Daresbury Laboratory for provision of facilities, the SERC for support (R. D. O.) and Drs. R. L. Bilsborrow and G. Van Dorssen for assistance with the EXAFS data collection.

References

1 W. Levason, M. D. Spicer and M. Webster, *Inorg. Chem.*, 1992, **31**, 2575.
2 D. B. Currie, W. Levason, R. D. Oldroyd and M. T. Weller, *J. Mater. Chem.*, 1993, **3**, 447.
3 D. B. Currie, W. Levason, R. D. Oldroyd and M. T. Weller, *J. Chem. Soc., Dalton Trans.*, 1994, 1483.
4 W. Levason, M. D. Spicer and M. Webster, *Inorg. Chem.*, 1991, **30**, 967.
5 W. Levason, M. D. Spicer and M. Webster, *J. Coord. Chem.*, 1991, **23**, 67.
6 W. Levason, M. D. Spicer and M. Webster, *J. Chem. Soc., Dalton Trans.*, 1988, 1377.
7 V. Adelskold, L. Eriksson, P.-L. Wang and P. E. Werner, *Acta Crystallogr., Sect. C*, 1988, **44**, 597.
8 A. M. El-Hendawy, W. P. Griffith, B. Piggott and D. J. Williams, *J. Chem. Soc., Dalton Trans.*, 1988, 1983.
9 R. Masse and A. Simon, *J. Solid State Chem.*, 1982, **44**, 201.
10 Y. Michiue, H. Ichida and Y. Sasaki, *Acta Crystallogr., Sect. C*, 1982, **43**, 175.
11 L. Lebioda, M. Ciechanowicz-Rutkowska, L. C. W. Baker and J. Growchowski, *Acta Crystallogr., Sect. B*, 1980, **36**, 2530.
12 A. C. Dengel, A. M. El-Hendawy, W. P. Griffith, S. I. Mostafa and D. J. Williams, *J. Chem. Soc., Dalton Trans.*, 1992, 3489.
13 R. Mattes and K.-L. Richter, *Z. Naturforsch., Teil B*, 1982, **37**, 1241.
14 A. Balikungeri, M. Pelletier and D. Monnier, *Inorg. Chim. Acta*, 1977, **22**, 7.
15 A. Balikungeri and M. Pelletier, *Inorg. Chim. Acta*, 1978, **29**, 137.
16 J. Evans, W. Levason and M. D. Spicer, *J. Chem. Soc., Dalton Trans.*, 1990, 2307.
17 G. M. Sheldrick, SHELXS 86, Program for solution of crystal structures, University of Göttingen, 1986; *Acta Crystallogr., Sect. A*, 1990, **46**, 467.
18 G. M. Sheldrick, SHELX 76, Program for crystal structure determination, University of Cambridge, 1976.
19 *International Tables for X-Ray Crystallography*, Kynoch Press, Birmingham, 1974, vol. 4.
20 W. D. S. Motherwell and W. Clegg, PLUTO, Program for plotting crystal and molecular structures, Universities of Cambridge and Göttingen, 1978.
21 N. Binsted, PAXAS, Program for the analysis of X-ray absorption spectra, University of Southampton, 1988.
22 N. Binsted, EXCURVE 92, SERC Daresbury Laboratory Program, 1992.
23 S. S. Hasnain (Editor), XAFS, Ellis Horwood, New York, 1991, ch. 195.
24 S. K. Harbron, H. C. Jewiss, W. Levason and M. Webster, *Acta Crystallogr., Sect. C*, 1987, **43**, 37.
25 C. Robl and M. Frost, *Z. Anorg. Allg. Chem.*, 1993, **619**, 1834.
26 O. Lindqvist and M. S. Lehmann, *Acta Chem. Scand.*, 1973, **27**, 85.
27 G. B. Johansson, O. Lindqvist and J. Moret, *Acta Crystallogr., Sect. B*, 1979, **35**, 1684.
28 A. Kalman and D. W. J. Cruickshank, *Acta Crystallogr., Sect. B*, 1970, **26**, 1782.
29 T. Kellersohn, *Acta Crystallogr., Sect. C*, 1991, **47**, 1133.
30 B. K. Teo, *EXAFS: Basic Principles and Data Analysis*, Springer, Berlin, 1986, ch. 5.

Received 31*st May* 1994; *Paper* 4/03223C